# Observation of exchange of micropore water in cement pastes by two-dimensional $T_2$-$T_2$ nuclear magnetic resonance relaxometry

L. Monteilhet,[1] J.-P. Korb,[2] J. Mitchell,[1] and P. J. McDonald[1,*]
[1]*Department of Physics,University of Surrey, Guildford, Surrey, GU2 7XH, United Kingdom*
[2]*Laboratoire de Physique de la Matière Condensée, UMR 7643 CNRS, Ecole Polytechnique, 91128 Palaiseau, France*
(Received 31 July 2006; published 22 December 2006)

The first detailed analysis of the two-dimensional (2D) NMR $T_2$-$T_2$ exchange experiment with a period of magnetization storage between the two $T_2$ relaxation encoding periods ($T_2$-store-$T_2$) is presented. It is shown that this experiment has certain advantages over the $T_1$-$T_2$ variant for the quantization of chemical exchange. New $T_2$-store-$T_2$ 2D $^1$H NMR spectra of the pore water within white cement paste are presented. Based on these spectra, the exchange rate of water between the two smallest porosity reservoirs is estimated for the first time. It is found to be of the order of 5 ms$^{-1}$. Further, a careful estimate of the pore sizes of these reservoirs is made. They are found to be of the order of 1.4 nm and 10–30 nm, respectively. A discussion of the results is developed in terms of possible calcium silicate hydrate products. A water diffusion coefficient inferred from the exchange rate and the cement particle size is found to compare favorably with the results of molecular-dynamics simulations to be found in the literature.

DOI: 10.1103/PhysRevE.74.061404 PACS number(s): 82.70.−y, 81.05.Rm, 68.08.−p, 78.30.Ly

## I. INTRODUCTION

Nuclear magnetic resonance (NMR) spin-lattice ($T_1$) and spin-spin ($T_2$) relaxation-time measurements have been shown to be a powerful tool for the characterization of liquids in porous media [1]. The fast exchange model of relaxation is often invoked and provides a powerful means of characterizing the pore surface-to-volume ratio. According to this theory, the observed relaxation rate is the weighted average of that for fast relaxing nuclei in molecules associated with pore surfaces and that for more abundant, but more slowly relaxing nuclei associated with molecules in the bulk liquid filling the pore [2]. In other work, NMR pulsed field gradient measurements of self-diffusion (D) of liquids in porous media and, in particular, of restricted diffusion, have been shown to be equally important for the characterization of pore structures [3]. More recently, two-dimensional relaxation correlation experiments, first suggested in the early 1980's [4], have come to the fore [5] following the availability of robust methods of performing the requisite 2D inverse Laplace transform [6]. In the usual form of these experiments, a measurement of $T_1$ made in a first measurement interval is correlated with a measurement of either $T_2$ or $D$ in an immediately following second interval. In particular, $T_1$-$D$ experiments have been shown to be well suited to the separation of signals from oil and water in reservoir rocks [7]. Others have applied the methods to the characterization of emulsions and foods [8,9]. The $T_2$-$T_2$ experiment is much less common and to date has not been part of this resurgence. However, it was first proposed more than a decade ago by Lee *et al.* [10]. The experiment is made useful by the inclusion of a magnetization storage period between the $T_2$ encoding periods, $T_2$-store-$T_2$, during which the magnetization is held along the longitudinal direction and during which exchange can occur.

Cement-based materials are a further significant class of porous materials. Understanding nanoscale pore-water interactions is important for both new build with fresh materials and for the repair of existing structures. With new build, for instance, knowledge of the degree of cure of cement is critical to the construction timeline. With regard to repair, it is accepted that nearly all forms of degradation of cement-based materials are ultimately linked to the availability of water and its transport through the porous structure.

Previous NMR relaxometry studies of cements have largely focused on simple measurements of $T_1$ and $T_2$ [11–13] and/or $D$ [14,15]. These measurements have generally shown three or more distinct relaxation reservoirs that are generally associated with chemically combined water (the shortest $T_2$) through water in the cement gel structures (CSH) and onto water in capillary pores and microcracks (the longest $T_2$). While the broad picture remains constant across these several reports, numerous factors conspire to leave considerable uncertainty in the overall interpretation. Amongst these are the variety of materials and water-to-cement ratios used; the varying cure regimes adopted and hence the varying degree of cure and saturation of porosities encountered; the different NMR spectrometer frequencies available; and the acknowledged difficulty of inverting spin-relaxation data to yield relaxation rates.

In an earlier paper [16] we showed that $T_1$-$T_2$ correlation experiments are valuable in helping to understand pore-water interactions in cement paste. Key findings included the following:

(i) confirmation of a series of discrete-sized porosity reservoirs;

(ii) the first observation of an off-diagonal peak linking relaxation of $^1$H in the two smallest porosity reservoirs. This was attributed to water exchange between the gel and capillary structures;

(iii) the observation that $T_1/T_2=\alpha$ is a constant greater than 1 across the full spectrum of relaxation times for water in different-sized pore structures;

*Corresponding author.

 

(iv) new analysis that extended a model of surface relaxation by a two-dimensional random walk of nuclei across a pore surface passed paramagnetic relaxation sinks [17]. This analysis satisfactorily explained the constant $\alpha$, and, by measurement of its frequency dependence [18], enabled an estimate of the pore surface residency time and the pore surface 2D walk hopping time, both consistent with previous measurements inferred from methodologically more complex field-cycling NMR experiments [19,20].

It is the purpose of this paper to carry this work forward, both in terms of the methodology and its analysis, and in terms of the interpretation of results in cements. For the first part, this paper focuses on analysis of the $T_2$-store-$T_2$ exchange experiment. Although in our previous paper we presented the first use of a $T_2$-store-$T_2$ exchange experiment for studying cement pastes, the application was not fully explored and only very preliminary results were included. It is now shown that this experiment has considerable advantages compared to a $T_1$-$T_2$ experiment for studying materials such as cements. New calculations show that 2D spectra with strong off-diagonal peaks can be observed unambiguously with a $T_2$-store-$T_2$ experiment in cases where there is ongoing exchange. Measurement of the relative intensity of the off-diagonal features as a function of the storage interval length permits an estimate of the exchange rate to be made. In the case of cement pastes this goes on to allow an estimate of water diffusivity within pore structures that can be compared to theoretical modelling.

## II. MATERIALS AND METHODS

Small samples of white Portland cement were carefully hand mixed in the water-to-cement ratio 0.4 by mass, cast into 10 mm NMR tubes, gently vibrated on a vibration table to remove entrapped air, and allowed to cure unsealed for the first few hours. As soon as the samples solidified, a small quantity of saturated $Ca(OH)_2$ aqueous solution (simulated pore-water) was poured onto the samples to allow continued cure underwater. This solution was temporarily removed during NMR measurements but replaced immediately thereafter. Notwithstanding this methodology, it is likely that a significant fraction of the open *capillary* porosity remained devoid of water since it is known that it is extremely hard to manufacture fully saturated samples. Samples were stored at 20 °C.

Samples were investigated with the $T_2$-store-$T_2$ exchange experiment, defined by the pulse sequence

$$P_{90}\text{-}(\beta^i\tau_{echo}\text{-}P_{180}\text{-}\beta^i\tau_{echo}\text{-echo-})_m\text{-}P_{90}\text{-}\tau_{delay}\text{-}P_{-90}\text{-}(\beta^j\tau_{echo}\text{-}P_{180}\text{-}\beta^j\tau_2\text{-echo-})_n\text{-}\tau_{RD}.$$

This experiment consists of three time intervals: $t_1$, $t_2$, and $t_3$. During the first interval a Carr-Purcell-Meiboom-Gill (CPMG) pulse train consisting of $m$ inversion pulses and echoes is applied. In our implementation, the inversion pulse gap increases throughout the sequence according to a geometric sequence ($2\beta^i\tau_{echo}, i=0,1,\ldots,m-1$ and $\beta$=constant) in order to span efficiently the entire range of relaxation times from tens of microseconds to seconds. At the end of the sequence, at the time of the $m_{\text{th}}$ echo, a 90° pulse is applied so as to store the magnetization along the $z$ axis. Phase cycling is used between averages so as to store along both $+/-z$ (see theory). The magnetization is stored for the period $\tau_{delay}=t_2$. Thereafter, the magnetization is recovered with a further 90° pulse. During the third period $t_3$, a second CPMG sequence of $n$ inversion pulses similarly spaced in geometric progression is applied and the series of echo intensities is recorded. The experiment is repeated for $m=1,2,\ldots,n$ with repetition delay $\tau_{RD}$. In this manner, a square two-dimensional relaxation data set is acquired.

Measurements were made at room temperature on a 20 MHz $^1$H NMR frequency Maran benchtop spectrometer (Oxford Instruments Molecular Biotools Ltd, Oxon, UK). The 90° pulse length was 2.5 $\mu$s. In a typical experiment, the inversion pulse gap interval of the CPMG sequence increased from 60 $\mu$s to 0.2 s over $n=32$ echoes so that the $T_2$ range up to circa 1 s was well explored. However, signal from the chemically combined water (with a $T_2$ of only a few microseconds) was not seen. The storage interval $t_2$ was kept constant in any one experiment and was of the order of 0–30 ms. As many as 128 averages of each echo train were recorded with a repetition time of 1 s in an experiment lasting circa 2.5 hours.

The 2D data sets were carefully phased prior to analysis. None of the data sets showed a noticeable baseline offset. Relaxation time distributions were extracted from the data by 2D Laplace inversion using the algorithm proposed by Venkataramanan *et al.* [21] using software running on a desktop computer. All subsequent data plots are as output by this algorithm except that intensities have been normalized to the number of averages recorded.

## III. THEORY

### A. $T_2$-store-$T_2$ experiment

We consider two reservoirs of magnetization, $M^a$ and $M^b$, corresponding to $^1$H (water) in pores of different sizes. There is exchange between the reservoirs. The system of coupled differential equations governing the relaxation of the magnetization in the reservoirs is well known [22], viz.,

$$\frac{dM_a}{dt} = -k_aM_a + k_bM_b + R_a(M_a^{eq} - M_a),$$

$$\frac{dM_b}{dt} = -k_bM_b + k_aM_a + R_b(M_b^{eq} - M_b), \quad (1)$$

where $k_{a,b}$ is the exchange rate, $R_{a,b}$ is the nuclear spin-lattice or spin-spin relaxation rate as appropriate, $M_{a,b}^{eq}$ is the equilibrium magnetization for each reservoir for the relevant process, and $t$ is time. For spin-lattice relaxation $M_{a,b}^{eq}=M_{a,b}^0$, the overall equilibrium value, while for spin-spin relaxation $M_{a,b}^{eq}=0$. The condition of detailed balance requires that $k_aM_a^0=k_bM_b^0$. Conveniently, under conditions of detailed balance, the equations can be written in the form

$$\begin{bmatrix} d(M_a - M_a^{eq})/dt \\ d(M_b - M_b^{eq})/dt \end{bmatrix} = \begin{bmatrix} -R_a - k_a & k_b \\ k_a & -R_b - k_b \end{bmatrix} \begin{bmatrix} M_a - M_a^{eq} \\ M_b - M_b^{eq} \end{bmatrix}. \tag{2}$$

The solutions to Eq. (2) are also well known [22] and have been presented previously in the notation of this work by us. [16] In order to treat the $T_2$-store-$T_2$ experiment, the time is divided into three periods, $t_1$, $t_2$, and $t_3$, corresponding to the three sequential elements of the experiment. The starting conditions are $M_{a,b}(0)=M_{a,b}^0$ and the magnetization $M_{a,b}(t_1)$ is calculated using spin-spin relaxation parameters [Eq. (10) of Ref. [16]]. $M_{a,b}(t_1)$ becomes the starting conditions for the second period. Hence, using spin-lattice relaxation parameters, the magnetization at the end of the second period, $M_{a,b}(t_1,t_2)$ is calculated. Likewise, $M_{a,b}(t_1,t_2)$ is the starting condition for period $t_3$ so that, finally, reverting to spin-spin relaxation parameters, $M_{a,b}(t_1,t_2,t_3)$ is calculated. The observed magnetization $M$ is the sum of $M_a$ and $M_b$. The final solution is given by

$$M(t_1,t_2,t_3) = C_1(t_3)[C_2(t_1,t_2) + C_3(t_1,t_2)] + C_4(t_3)[C_5(t_1,t_2) + C_6(t_1,t_2)], \tag{3}$$

where

$$C_1(t_3) = (A_2^- - F_2)\exp(s_2^+ t_3) + (A_2^+ + F_2)\exp(s_2^- t_3), \tag{4}$$

$$C_2(t_1,t_2) = M_a^0 + [A_1^- \exp(s_1^+ t_2) + A_1^+ \exp(s_1^- t_2)] \times [-M_a^0 + (A_2^- M_a^0 - G_2 M_b^0)\exp(s_2^+ t_1) + (A_2^+ M_a^0 + G_2 M_b^0)\exp(s_2^- t_1)], \tag{5}$$

$$C_3(t_1,t_2) = -G_1[\exp(s_1^+ t_2) - \exp(s_1^- t_2)] \times [-M_b^0 + (B_2^- M_b^0 - F_2 M_a^0)\exp(s_2^+ t_1) + (B_2^+ M_b^0 + F_2 M_a^0)\exp(s_2^- t_1)], \tag{6}$$

and where

$$s_{1,2}^{+/-} = -\frac{R_a^{1,2} + k_a + R_b^{1,2} + k_b}{2} \pm \frac{1}{2}\sqrt{(R_a^{1,2} + k_a + R_b^{1,2} + k_b)^2 - 4[(R_a^{1,2} + k_a)(R_b^{1,2} + k_b) - k_a k_b]}, \tag{7}$$

$$A_{1,2}^{+/-} = \frac{s_{1,2}^{+/-} + R_a^{1,2} + k_a}{s_{1,2}^{+/-} - s_{1,2}^{-/+}}, \tag{8}$$

$$B_{1,2}^{+/-} = \frac{s_{1,2}^{+/-} + R_b^{1,2} + k_b}{s_{1,2}^{+/-} - s_{1,2}^{-/+}}, \tag{9}$$

$$F_{1,2} = \frac{k_a}{s_{1,2}^- - s_{1,2}^+}, \tag{10}$$

and

$$G_{1,2} = \frac{k_b}{s_{1,2}^- - s_{1,2}^+}. \tag{11}$$

Expressions for $C_4$, $C_5$, and $C_6$ are found by interchanging $a$ and $b$ throughout $C_1$, $C_2$, and $C_3$, respectively. Finally, $R_a^1 = 1/T_{1a}$, for example, is the spin-lattice relaxation rate for reservoir $a$.

The solution can be rewritten as a sum of products including factors $\exp(s_2^{+/-}t_1)\exp(s_2^{+/-}t_3)$ and other terms not including these factors. The amplitudes of terms involving factors of $\exp(s_2^{+/-}t_1)\exp(s_2^{+/-}t_3)$ correspond to the intensities of the diagonal, $P^{++}$ and $P^{--}$ and off-diagonal, $P^{+-}$ and $P^{-+}$ peaks in the 2D Laplace inversion of the magnetization. The other terms are an unwanted distraction and are conveniently removed by phase cycling. Experimentally, the magnetization is stored along the $+z$ and $-z$ axes during $t_2$. Theoretically, the calculation is repeated using $-M_{a,b}(t_1)$ at the start of the second period. The results of the two variants are summed whereupon the unwanted terms cancel to zero leaving just those wanted. The resultant amplitudes are

$$P^{++} = \exp(s_1^+ t_2)\{(A_2^- - F_2)[A_1^-(A_2^- M_a^0 - G_2 M_b^0) - G_1(B_2^- M_b^0 - F_2 M_a^0)] + (B_2^- - G_2)[B_1^-(B_2^- M_b^0 - F_2 M_a^0) - F_1(A_2^- M_a^0 - G_2 M_b^0)]\} + \exp(s_1^- t_2)\{(A_2^- - F_2)[A_1^+(A_2^- M_a^0 - G_2 M_b^0) + G_1(B_2^- M_b^0 - F_2 M_a^0)] + (B_2^- - G_2)[B_1^+(B_2^- M_b^0 - F_2 M_a^0) + F_1(A_2^- M_a^0 - G_2 M_b^0)]\}, \tag{12}$$

$$P^{--} = \exp(s_1^+ t_2)\{(A_2^+ + F_2)[A_1^-(A_2^+ M_a^0 + G_2 M_b^0) - G_1(B_2^+ M_b^0 + F_2 M_a^0)] + (B_2^+ + G_2)[B_1^-(B_2^+ M_b^0 + F_2 M_a^0) - F_1(A_2^+ M_a^0 + G_2 M_b^0)]\} + \exp(s_1^- t_2)\{(A_2^+ + F_2)[A_1^+(A_2^+ M_a^0 + G_2 M_b^0) + G_1(B_2^+ M_b^0 + F_2 M_a^0)] + (B_2^+ + G_2)[B_1^+(B_2^+ M_b^0 + F_2 M_a^0) + F_1(A_2^+ M_a^0 + G_2 M_b^0)]\}, \tag{13}$$

$$P^{-+} = P^{+-} = \exp(s_1^+ t_2)\{(A_2^+ + F_2)[A_1^-(A_2^- M_a^0 - G_2 M_b^0) - G_1(B_2^- M_b^0 - F_2 M_a^0)] + (B_2^+ + G_2)[B_1^-(B_2^- M_b^0 - F_2 M_a^0) - F_1(A_2^- M_a^0 - G_2 M_b^0)]\} + \exp(s_1^- t_2)\{(A_2^+ + F_2)[A_1^+(A_2^- M_a^0 - G_2 M_b^0) + G_1(B_2^- M_b^0 - F_2 M_a^0)] + (B_2^+ + G_2)[B_1^+(B_2^- M_b^0 - F_2 M_a^0) + F_1(A_2^- M_a^0 - G_2 M_b^0)]\}. \tag{14}$$

In the event that $T_1=T_2$, then the off-diagonal peak intensities evaluate to zero. However, experimental work suggests

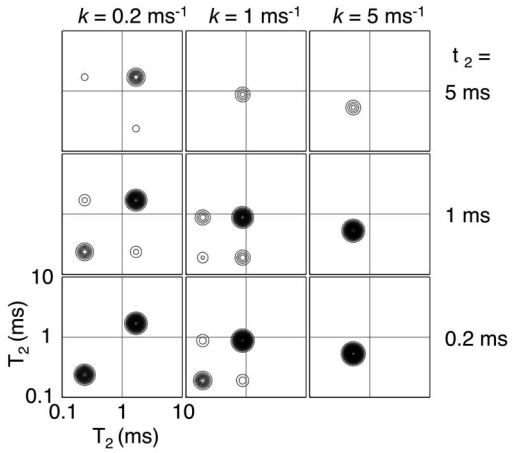


FIG. 1. Calculated 2D $T_2$-store-$T_2$ spectra for (left to right) slow, medium, and fast exchange rates and (bottom to top) short, intermediate, and long storage times. Calculation parameters are given in the text. The plots are on a common scale with the contours spaced at 1.5% of the total magnetization intensity.

that, in cements as in some other porous media, $T_1 \neq T_2$. In our previous work on cements at a Larmor frequency of 20 MHz we observed two principal relaxation reservoirs of comparable volume differing in $T_1$ by a factor of approximately ten each with $T_2$ a factor of 4 smaller. The common $T_1/T_2$ ratio of 4 is discussed further in the next section. Here we focus on how the four peak intensities vary with the storage time $t_2$ for different exchange rates.

We have performed numerical calculations with $M_a^{eq}=M_b^{eq}=0.5$ and $T_{2a}=T_{1a}/4=0.25$ ms and $T_{2b}=T_{1b}/4=2.5$ ms. For reservoirs of equal size, $k_a=k_b=k$. Figure 1 shows simulated 2D correlation spectra for each of "slow," "medium," and "fast" exchange rate ($k=0.2$, 1.0, and 5.0 $\text{ms}^{-1}$, respectively) with a "short," "intermediate," and "long" storage interval ($t_2=0.2$, 1, and 5 ms, respectively). The terms slow and long etc. are defined relative to the difference in the spin-lattice relaxation rates. The calculated spectral peaks are delta functions: they have been artificially broadened for the sake of pictorial clarity. The contour plots are all shown on the same vertical scale, relative to a zero baseline, and are directly comparable.

With slow exchange and only a short storage interval [Fig. 1 (bottom left)], then the spectrum consists essentially of two strong diagonal peaks $P^{++}$ and $P^{--}$, of comparable amplitude and located close to the intersections $(T_2,T_2)=(0.25,0.25)$ and (2.5,2.5) where $T_2$ is expressed in ms, as expected. In the limit $k\rightarrow 0$ and $t_2\rightarrow 0$ the peaks are of equal amplitude and centered exactly on these intersects. With increasing exchange rate (bottom center) the two diagonal peaks start to drift and change in relative intensity such that one becomes dominant in the expected fashion. Additionally, two off-diagonal peaks $P^{+-}$ and $P^{-+}$ appear as the signature of the ongoing exchange. With fast exchange (bottom right), only one diagonal peak is seen at a location (0.45,0.45), determined by the average $T_2$ relaxation rate. The off-diagonal peaks are no longer seen. As the storage time increases (from the bottom to the top of Fig. 1), so the integrated intensity across the four peaks declines due to spin-lattice relaxation

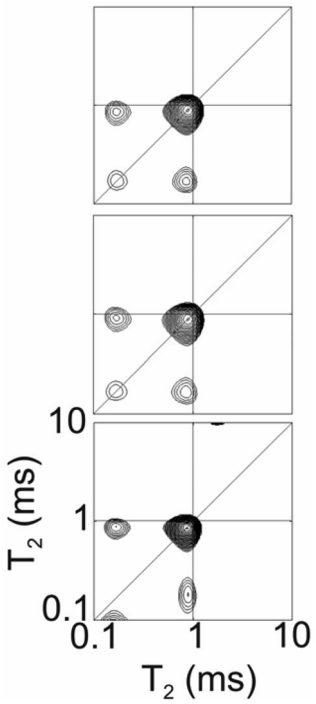


FIG. 2. Laplace inversions of simulated NMR data sets with (top) no noise, (middle) 2% white noise, and (bottom) 2% white noise plus 1% baseline offset. These plots have the same initial parameters as the center plot of Fig. 1 ($k=1$ $\text{ms}^{-1}$, $t_2=1$ ms).

losses. This is particularly true for the lower diagonal peaks that have short $T_2$ and hence correspondingly short $T_1$. It is also true, however, that the fraction of the spectral intensity in the off-diagonal peaks increases.

In order to assess how the Laplacian inversion affects data, we have simulated NMR signals and added noise and systematic errors and subjected these to the 2D inverse Laplace transform for comparison with Fig. 1. The simulated signals were generated with $k=1$ $\text{ms}^{-1}$, $t_2=1$ ms, $T_2^a=0.25$ ms, $T_2^b=2.5$ ms, and $T_1/T_2=4$. In the absence of added noise, it can be seen, with reference to Fig. 2 (top), that the positions of the peaks obtained by this method are almost identical to those obtained by direct numerical simulation [Fig. 1 (center)]. A comparison of the integrated peak intensities with the direct numerical simulations reveals an absolute error of 3% in the intensity of the off-diagonal peaks. This translates to a relative error of 15% in the fraction of the intensity appearing in the off-diagonal peaks. The inclusion of 2% white noise [Fig. 2 (middle)], made a marginal further difference to the inversion. However, the addition of 1% baseline offset [Fig. 2 (bottom)], distorted the plot, forcing the $P^{--}$ peak to lower values of $T_2$.

Figure 3 shows the calculated intensity within the off-diagonal peaks $I_{OD}$, relative to the total signal intensity $I_{TOT}$,

$$\frac{I_{OD}}{I_{TOT}}=\frac{P^{+-}+P^{+-}}{P^{++}+P^{-+}+P^{+-}+P^{--}}, \tag{15}$$

plotted as a function of storage ($t_2$) and exchange time ($\tau=1/k$) for $T_{1a}=4T_{2a}=1$ ms and $T_{1b}=4T_{2b}=7.1$ ms. It is clear

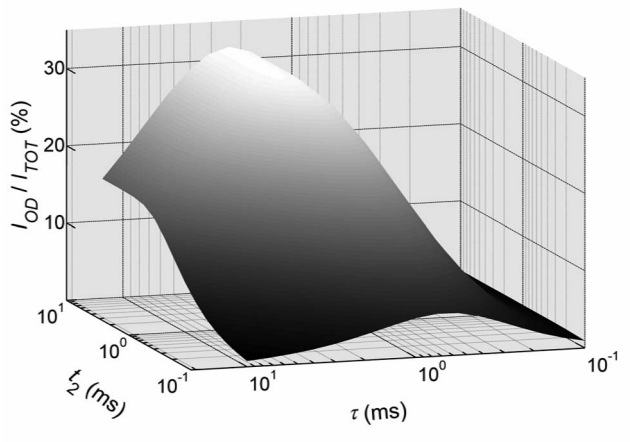


FIG. 3. A surface plot showing the fraction of the observed spectral intensity in the off-diagonal peaks as a function of exchange time $\tau=1/k$, and storage time $t_2$. The calculation parameters are given in the text.

that, under favorable conditions, as much as 30% of the magnetization can appear in the off-diagonal peaks.

### B. Surface relaxation

The observed spin-spin relaxation time $T_2^{OBS}$ can be related to a pore surface-to-volume ratio ($S/V$; pore size) through the well-known equation

$$\frac{1}{T_2^{OBS}} = \frac{\lambda S}{V}\frac{1}{T_2^S}, \tag{16}$$

where $T_2^S$ is the relaxation time for $^1$H in molecules adsorbed on the pore surface and $\lambda$ is the thickness of a surface layer. In Eq. (16), the contribution of the bulk spin-spin relaxation rate has been eliminated due to its very small value. A key issue is to evaluate $T_2^S$. In our previous work [16,17,19], a model for surface relaxation was proposed and shown to be applicable. The model supposes biphasic fast exchange between liquid molecules that are transiently adsorbed on the pore surface and molecules in the bulk pore liquid phase. The adsorbed molecules relax as they undergo 2D translational diffusion in the dipolar field of the electronic spins fixed at the pore surface. The frequency dependence of this relaxation has been carefully evaluated. It depends on two correlation times, namely, the correlation time $\tau_m$ of surface diffusion events and a finite residence time $\tau_s$ of the protons on the surface. In most cases $\tau_m/\tau_s \ll 1$. In the case of $T_2$, the model analysis yields the result

$$\frac{1}{T_2^S} = \frac{4}{9}\gamma_I^2\gamma_S^2\hbar^2 S(S+1)\left\{J_L^0(0) + \frac{1}{4}J_L^0(\omega_I-\omega_S) + \frac{3}{4}J_L^1(\omega_I) + \frac{3}{2}J_L^1(\omega_S) + \frac{3}{2}J_L^2(\omega_I+\omega_S)\right\}, \tag{17}$$

where $\gamma_S$ and $\gamma_I$ are the gyromagnetic ratio of the electron and proton, respectively, $S$ is the spin of the paramagnetic impurities ($Fe^{3+}$) embedded in the pore surface, and $\omega_S$ and $\omega_I$ are the electron and proton resonant frequencies, and where

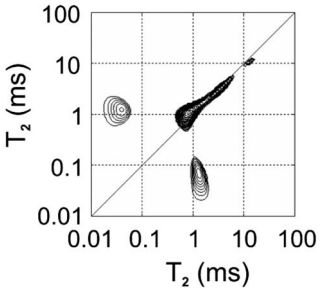


FIG. 4. Experimental $T_2$-store-$T_2$ 2D correlation spectrum for a white cement paste with water-to-cement ratio 0.4 and three days old. The storage time is 10 ms. The spectrum, which shows a strong upper diagonal peak and two off-diagonal peaks, is qualitatively comparable to the central part of Fig. 1.

$$J_L^{0,1,2}(\omega) = \frac{3}{40}\frac{\pi\sigma_s}{\delta^4}\tau_m \ln\left[\frac{1+\omega^2\tau_m^2}{\left(\frac{\tau_m^2}{\tau_s^2}\right)+\omega^2\tau_m^2}\right]. \tag{18}$$

Here, $\sigma_S$ is the surface density of paramagnetic impurities and $\delta$ is the distance of minimum approach of the water $^1$H to the paramagnetic ($Fe^{3+}$) ions. The result can be simplified using the inequality $\omega_S \gg \omega_I (\omega_S = 658.21\omega_I)$. In the case of spherical pores, $S/V=6/d$, where $d$ is the pore diameter and $\lambda = x\epsilon$ where $x$ is the number of adsorbed water molecules of diameter $\epsilon$ in the surface layer. For planar pores, such as might better characterize CSH gel structures, $S/V=2/d$, where $d$ is the pore width.

A similar analysis has been performed for $T_1$ from which the ratio $T_1/T_2$ is calculated. For a fixed Larmor frequency, the value achieved for $T_1/T_2$ is not universal but depends critically on the ratio $\tau_m/\tau_s$. In particular, $T_2/T_1$ reaches the value 4 when $\tau_m/\tau_s = 10^{-3}$. What is important in our 2D $T_1$-$T_2$ data used to underpin the modeling in the previous section, is the strong correlation of all the discrete pore size distribution features along the line $T_1/T_2=4$. Given that paramagnetic impurities are expected to be distributed uniformly throughout the solid matrix of the sample, this provides strong supportive evidence for the surface diffusion model of proton nuclear spin relaxation in cements. Further support comes from the predicted frequency dependence of this ratio, which agrees well with experimental results [18].

## IV. EXPERIMENTAL RESULTS

### A. 2D correlation experiments

Figure 4 shows the results of an experiment to measure $T_2$-store-$T_2$ correlations in a white cement sample 4 days old. In this case, the storage interval was 10 ms. The spectrum shows a clear diagonal ridge with a primary peak $P^{++}$ at circa $(T_2,T_2)=(1,1)$ and two strong off-diagonal peaks $P^{+-}$ and $P^{-+}$ at circa (0.05,1) and (1,0.05), respectively. There is no evidence for the second lower diagonal feature $P^{--}$ and so, superficially at least, the spectrum is comparable to that in the upper left of Fig. 1.

Figure 5 shows a second example. In this case the storage time is reduced to 1 ms. Now, overall, there is considerably

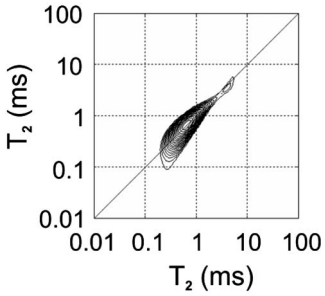


FIG. 5. Experimental $T_2$-store-$T_2$ 2D correlation spectrum for a white cement paste with water-to-cement ratio 0.4 and four days old. The storage time is 1 ms. Compared to Fig. 3, the contour spacing is 10× greater: the maximum intensity is almost 10× as great. The spectrum, which shows a strong diagonal ridge, is qualitatively comparable to the lower left/central parts of Fig. 1.

more intensity in the spectrum (notice the expansion of the contour interval). However, it is located predominantly along the diagonal. The off-diagonal features are not seen. The spectrum is more comparable to the lower left of Fig. 1. The slight asymmetry in this spectrum could be due to one of several causes including ongoing hydration of the sample during the measurement introducing systematic error or failure of the Laplace inversion.

To check the efficacy of the pulse sequence, a $T_2$-store-$T_2$ experiment with a store time $t_2=5$ ms was performed on a four-day-old sample of white cement. The experiment was repeated with the first 90° pulse of the sequence suppressed. In the latter case, the signal intensity echo showed no signal arising from unwanted coherences visible above the baseline noise. Equally, the inverse Laplace transform spectrum showed no clear structural features. The ratio of the integrated intensity of the spectra between the two experiments was $<0.4\%$, well below the amplitude associated with the exchange peaks where they occur. We are therefore confident that the observed exchange peaks are not an artifact of the pulse sequence implementation.

Figure 6 shows the fractional intensity in the off-diagonal peaks as a function of storage time for all the white cement samples of age four days and water-to-cement ratio 0.4 that have so far been surveyed in our laboratory. The circles are for data recorded in the experiments discussed here. The triangles are for earlier preliminary experiments where the signal-to-noise ratio was not as good. Also, the cement powder used was from a different (older) batch and the sample storage was not as carefully controlled as here. As expected, it is found that the fractional intensity in the off-diagonal features increases with storage time. However, since the overall signal intensity is declining, so the measurement error also increases. The error bars have been obtained as follows. The standard deviation of the baseline signal in the tail of the raw data was calculated. Gaussian white noise of the same standard deviation was generated artificially and added to the raw data. The modified data was inverted and the peak intensities and ratios recalculated. The process was repeated several times and the standard deviation of the resultant peak intensities and ratios was thus calculated and taken as an estimate of the experimental error. It is noted that even after

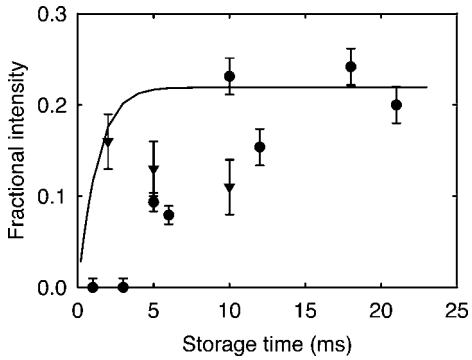


FIG. 6. The integrated intensity in the off-diagonal peaks of measured 2D spectra as a fraction of the total intensity as a function of storage time for white cement paste samples four days old with water-to-cement ratio 0.4. The solid line is a numerical calculation according to the theory developed in Sec. III A. The symbols are data for two series of experiments. The parameters are given in the text, Sec. IV A.

consideration of the errors in this way, there remains considerable scatter in the data. There are at least two potential reasons for this. First, at four days, the cement is still hydrating and the microstructure rapidly developing during the course of the measurement. This is in strong contrast to other porous media often studied by these methods, such as rock cores. This could lead to systematic error. Moreover, when two measurements at different storage times are made on the same sample, the measurements are necessarily for differently aged samples. If two samples are used, then they may be significantly different due to the mechanical mixing and natural sedimentation and bleeding of the cement. Second, as shown in Sec. III A, noise in the data and particularly a residual baseline offset can systematically affect the Laplace inversion and hence the measured peak intensity ratio.

The solid line in Fig. 6 is an attempt to fit the theory of Sec. III A to the data. A least-squares analysis has not been possible due to the very large number of unknown parameters and the fact that the sample almost certainly contains a distribution of pore sizes. The fit shown is based upon two reservoirs of equal volume, as justified below, with $T_2$ relaxation times of 250 $\mu$s and 1.8 ms, respectively and corresponding $T_1$ relaxation times four times longer. The exchange rate $k$ is 0.2 $\text{ms}^{-1}$. The analysis tends to overestimate the rate of increase in the off-diagonal magnetization with increased storage time. This is not readily overcome by varying the parameters within acceptable limits: better fits can only be achieved by using unrealistically long $T_1$ and $T_2$ times. However, without improved data, which our experience shows is very difficult to obtain, this discrepancy is not readily resolved.

Finally, Fig. 7 shows the total spectral intensity and the fraction of this intensity contained within the bottom left corner spectral features (i.e., that corresponding to the smallest and next-smallest pore-size porosity reservoirs) as a function of the sample age for white cement pastes with a water-to-cement ratio of 0.4. These data are extracted from $T_1$-$T_2$ correlation experiments of the sort previously described rather than $T_2$-store-$T_2$ experiments because the $T_1$-$T_2$ ex-

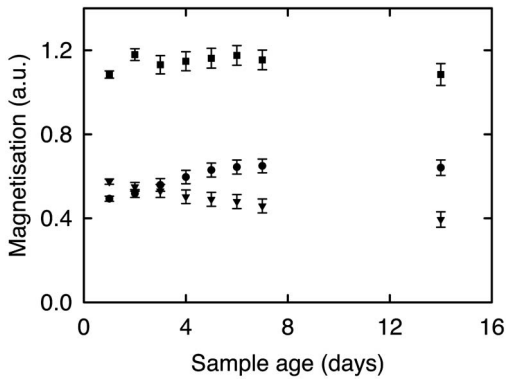


FIG. 7. The signal intensity (squares) and intensity within the fraction representing the smallest (circles) and next-smallest (triangles) pore-size porosity reservoirs as a function of curing time for a white cement paste with a water-to-cement ratio of 0.4. The data are evaluated from $T_1$-$T_2$ correlation experiments of the sort previously described, rather than $T_2$-store-$T_2$ correlations to minimize the complications of exchange averaging.

periment is better for quantization of the intensity of the lower diagonal peak corresponding to the smallest pores. It is seen that the total magnetization remains constant within experimental error throughout the curing period from 1 to 14 days. This suggests that the total water-filled porosity is not varying greatly. Over 95% of the magnetization is found in the spectral features corresponding to reservoirs of the two smallest pores. Of this magnetization, the fraction occurring in the smallest gel pores increases from circa 45% to 62% over the same period. This is consistent with the growth of CSH gel phase. The two small pore reservoirs are of approximately equal magnitude after three days, thereby justifying the use of reservoirs of equal volume in the previous analysis.

### B. Measurement of the pore size

Table I gives estimates of the parameters required to calculate the principal characteristic pore sizes in the measured cements using Eq. (16)–(18) along with the origin of these estimates. The experimentally measured values of the two principal relaxation reservoirs $T_2^{OBS}$ are circa 300 $\mu$s and 2.0 ms. If the smaller pores are planar as seems reasonable for CSH gel structures, then the water layer is calculated to be 1.0+/− 0.3-nm-thick. The larger pore shape is less certain. If it is planar, then the most likely size is 6+/−2 nm; if spherical then the diameter is 19+/−6 nm. The significance of these sizes is discussed in Sec. V B. Here we focus on the measurement accuracy. The uncertainties in the above analysis are based on the uncertainties in the parameters given in Table I, including $T_2^{OBS}$, but excluding $\delta$, the distance of closest approach of the water $^1$H to the ferric ions and $x$, the effective number of water molecules in the surface layer. The analysis is sensitive to both of these values. Careful inspection of the intermediate, values leading to these results suggests two related difficulties. The first is that $2x\epsilon$, the combined thickness of the two surface layers on either side of a planar pore exceeds the pore thickness. The second is that the surface relaxation time $T_2^S$=520 $\mu$s exceeds the smallest value of $T_2^{OBS}$=300 $\mu$s. Both results are physically unrealistic. If the calculation is repeated for smaller values of $\delta$ =0.20 nm and a monosurface layer $x$=1, then the pore size is increased only slightly, as the two changes largely cancel. The small planar pore spacing evaluates to 1.6+/−0.3 nm thick, for instance. However, a physically realistic value of $T_2^S$=100 $\mu$s is found and the surface layers fit within the pore. A distance of minimum approach $\delta$=0.2 nm between the proton and the ferric ions on the surface is greater than half of the water molecule diameter. However, it is known that water has extensive hydrogen bonding capabilities and may exchange protons with other surface sites. It may be-

TABLE I. Best estimates of the parameters required to calculate the pore size from the observed NMR relaxation times.

| Parameter | Best estimate | Uncertainty | Source |
|---|---|---|---|
| $\sigma_s$ | $2.5\times10^{11}$ $Fe^{3+}$ $cm^{-2}$ | ±20% (model dependent) | Calibrated ESR experiment on this cement following method of Ref. [19] |
| $\delta$ | 0.3 nm | +20/−100% | See text, Sec. IV B; Ref. [19] |
| $\tau_m$ | 1.3 ns | ±0.3 ns | Field cycling NMR, Ref. [19] |
| $\tau_s$ | 13 $\mu$s | ±5 $\mu$s | $T_1$-$T_2$ NMR correlations, Refs. [16,18] |
| $x$ | 1–3 | see text, Sec. IV B | Refs. [23,24] |
| $\epsilon$ | 0.28 nm | ±5% | Ref. [25] |
| $T_2^{OBS}$ | | | |
| Large | 2000 $\mu$s | ±10% | This work in the short $t_2$ limit and $T_1$-$T_2$ correlations, Ref. [16] |
| Small | 300 $\mu$s | ±10% | |

have as both a Lewis acid or base and generally coordinates to most metal ions. Hence it is very plausible that there are labile-OH proton species at such a small distance from the ferric ions. We have studied elsewhere [26] the anomalous surface dynamics of water in nanoporous silica glasses and have considered in detail the local geometry of minimal approach of a proton species to a ferric ion.

## V. DISCUSSION

### A. 2D correlation experiments

The $T_2$-store-$T_2$ experiment has been shown to give 2D relaxation spectra from white cement pastes with considerable information content. The storage period is critical to the experiment. Without it ($t_2=0$) the experiment collapses into no more than a conventional CPMG experiment, albeit with the data collected and presented in an unusual fashion. As such, the inverted 2D spectrum is expected to be entirely diagonal and to contain no additional information over its 1D counterpart. This has been confirmed experimentally by the appropriate analysis of a 1D data set although the trivial result is not shown here. The $t_2$ interval breaks the inherent symmetry of the experiment and yields off-diagonal peaks in the presence of exchange so long as $T_1 \neq T_2$. With small storage time, the fractional intensity in the off-diagonal elements is small. As $t_2$ gets longer, so the relative intensity in these peaks increases. However, the overall integrated intensity in the spectrum decreases due to spin-lattice relaxation losses occurring during $t_2$. The $T_2$-store-$T_2$ experiment has two significant advantages over the $T_1$-$T_2$ experiment, which was the focus of our previous work. First, the new experiment more clearly identifies and correlates measurements in two intervals $t_1$ and $t_3$ that are separated in time by a third interval, $t_2$. It is therefore more straightforward to consider that there is an exchange period during which the $^1$H are moving between reservoirs. Second, the off-diagonal peaks can be assigned unambiguously to exchange. If there is no exchange, then there are no off-diagonal peaks. In the case of the $T_1$-$T_2$ experiment, theory shows that the off-diagonal peaks are antisymmetric. However, the fast Laplace inversion algorithm does not detect the negative peak and leaves the ambiguity that the sole surviving positive off-diagonal peak may be due to a further $^1$H reservoir with $T_1 \neq T_2$, perhaps a solid component. As an aside, we note that we previously suggested on the basis of preliminary results [16] that the off-diagonal peaks in the $T_2$-store-$T_2$ experiment become asymmetric as $t_2$ increases due to the $T_1$ weighting. This is now seen as erroneous from both the theoretical and experimental points of view. Equation (3) shows that the off-diagonal peaks should be symmetric; equally, the further and improved data such as is shown in Figs. 4 and 5 suggest that this is true. The $T_2$-store-$T_2$ experiment is not always to be preferred over $T_1$-$T_2$. Empirically, we find that the $T_1$-$T_2$ experiment is better for the quantization of the intensity of the lower diagonal peak; hence this experiment was used to generate the data needed for Fig. 7.

### B. Measurement of the pore size

The calibration of the pore sizes suggests that the two primary relaxation reservoirs seen both comprise rather small pores. The smallest pore size is circa 1.0–1.7 nm. This is consistent with estimates to be found in the literature of the CSH interplanar spacing, which range from 0.9 to 1.4 nm [27]. However, the second significant reservoir suggests a size ranging from 7 to 30 nm, dependent on pore shape and details of the surface water layer. This is much smaller than the expected size of capillary pores. We therefore now suggest that the two observed reservoirs may be attributed to alternate gel structures. One possibility is that the smaller pore-size reservoir is associated with the inner product, the larger with the outer product, both created as the material hydrates. An alternate possibility is that the smaller-sized pores are associated with the intersheet spacing within CSH and the larger with the spaces between the packets of CSH sheets comprising the gel, but still much smaller than the normally accepted capillary porosity. This discussion will be expanded in a future discussion of results obtained from specific and otherwise (e.g., by electron microscopy, etc.) well-characterized CSH phases such as alite. For the time being we make just the following observations. The lack of directly observed capillary water in larger pores is not inconsistent with the methodology of preparation of the samples. The samples are exposed to air for the first 12 h of cure, and although they are subsequently stored underwater, any open capillary porosity is likely to remain unfilled except at the sample surface.

Figure 7 suggests that the total volume of water-filled porosity within our samples is not changing with time. This is consistent with the known sample history where, although the samples are cured underwater from age $\approx$12 h onward, the mobile water content is unlikely to be changing significantly. However, Fig. 7 further shows that the distribution of water between the different internal reservoirs is changing. There is a clear increase in the fraction of water associated with the smallest calcium silicate hydrate (CSH) pores during the first 14 days. This is consistent with a growth of CSH.

### C. Water diffusivity

Finally, the data presented in Fig. 5 suggest an empirical exchange time of circa 5 ms between the two porosity reservoirs. The particle-size distribution of the cements used in this study is strongly centered on a radius $r=7.5$ $\mu$m. A typical length scale between inner and outer product within a hydrating grain will therefore be $r/2 \approx 4$ $\mu$m. A diffusion coefficient can be calculated from this time ($t=5$ ms) and distance ($a=r/2=4$ $\mu$m) using the Einstein equation

$$D = \frac{\langle a^2 \rangle}{6t}. \tag{19}$$

The result is $5 \times 10^{-10}$ m$^2$ s$^{-1}$. In this simple analysis, issues such as tortuosity have not been considered and will be significant. Moreover, it is not clear exactly what the length scale corresponds to, since it is not yet clear exactly where the water is moving from and to. Nonetheless, the value of $D$ obtained is remarkably similar to that calculated by Kalinichev *et al.* [28] using molecular dynamics simulations for water diffusing in the pore space above the internal pore

surface of tobermorite, another mineral phase closely related to CSH. They obtain $6.0\times10^{-10}$ m$^2$ s$^{-1}$.

We have previously pointed out that a surface diffusion coefficient based on a length derived from the size of a water molecule ($a=\epsilon=0.3$ nm) and our previous measurements of a surface hopping time ($t=\tau_m=1$ ns) yield a diffusivity[1] $D=2.3\times10^{-11}$ m$^2$ s$^{-1}$. This value is in good agreement with the value of $5.0\times10^{-11}$ m$^2$ s$^{-1}$ obtained by Kalinichev *et al.* for water diffusing on the internal pore surfaces of tobermorite, again by molecular dynamics simulation. This double coincidence of agreement between diffusivities clearly warrants further investigation.

## VI. CONCLUSION

We have presented the first detailed analysis of the NMR $T_2$-store-$T_2$ 2D correlation-relaxation experiment and shown that it has certain advantages over the $T_1$-$T_2$ variant previously studied. Experimental results for curing white cement pastes have revealed new information about the water dynamics within the cement nanopores. The principal pore sizes of two porosity reservoirs have been carefully estimated and attributed to different structures with the CSH gel. For the first time, the exchange rate between these structures has been estimated. It is circa 5 m s$^{-1}$. From this, the water diffusivity within the CSH gel has been calculated and found to broadly correspond to the results of molecular-dynamic simulations in related systems to be found in the literature.

[1]Note that the factor 6 needs to be replaced by a factor 4 in the Einstein equation for a 2D walk.

## ACKNOWLEDGMENTS

The authors thank K. Scrivener of Ecole Polytechnique Federale de Lausanne for helpful discussions related to the interpretation of the relaxation reservoirs and for providing a particle-size distribution analysis of the cement powder used in this study, Y.-Q. Song of Schlumberger-Doll Research for the use of a copy of his 2D Fast Laplace Inversion software, and M. Mulheron of The University of Surrey for useful discussions and advice on making the samples. L.M. thanks the Nanocem Consortium for financial support. J.M. thanks The Royal Society for financial support.

[1] P. J. Barrie, Annu. Rep. NMR Spectrosc. **41**, 265 (2000).
[2] K. R. Brownstein and C. E. Tarr, Phys. Rev. A **19**, 2446 (1979).
[3] P. T. Callaghan, *Principles of Nuclear Magnetic Resonance Microscopy* (Oxford, Clarendon Press, 1991).
[4] H. Peemoeller, R. K. Shenoy, and M. M. Pintar, J. Magn. Reson. **45**, 193 (1981).
[5] Y. Q. Song, L. Venkataramanan, and M. D. Hurlimann, J. Magn. Reson. **154**, 261 (2002).
[6] L. Venkataramanan, Y. Q. Song, and M. D. Hürlimann, IEEE Trans. Signal Process. **50**, 1017 (2002).
[7] M. D. Hürlimann, M. Flaum, L. Venkataramanan, C. Flaum, R. Freedman, and G. J. Hirasaki, Magn. Reson. Imaging **21**, 305 (2003).
[8] S. Godefroy and P. T. Callaghan, Magn. Reson. Imaging **21**, 381 (2003).
[9] B. Hills, S. Benamira, N. Marigheto, and K. Wright, Appl. Magn. Reson. **26**, 543 (2004).
[10] J. H. Lee, C. Labadie, C. S. Springer, and G. S. Harbison, J. Am. Chem. Soc. **115**, 7761 (1993).
[11] L. J. Schreiner, J. C. MacTavish, L. Miljkovic, M. M. Pintar, R. Blinc, G. Lahajnar, D. D. Lasic, and L. W. Reeves, J. Am. Ceram. Soc. **68**, 10 (1985).
[12] D. D. Lasic, J. M. Corbett, J. Jian, J. C. MacTavish, M. M. Pintar, R. Blinc, and G. Lahajnar, Cem. Concr. Res. **18**, 649 (1988).
[13] J. Greener, H. Peemoeller, C. Choi, R. Holly, E. J. Reardon, C. M. Hansson, and M. M. Pintar, J. Am. Ceram. Soc. **83**, 623 (2000).
[14] K. Friedemann, F. Stallmach, and J. Kärger, Cem. Concr. Res. **36**, 817 (2006).
[15] E. W. Hansen, H. C. Gran, and E. Johannessen, Microporous Mesoporous Mater. **78**, 43 (2005).
[16] P. J. McDonald, J.-P. Korb, J. Mitchell, and L. Monteilhet, Phys. Rev. E **72**, 011409 (2005).
[17] J.-P. Korb, M. Whaley-Hodges, and R. G. Bryant, Phys. Rev. E **56**, 1934 (1997).
[18] P. J. McDonald, J. Mitchell, M. Mulheron, P. S. Aptaker, J.-P. Korb, and L. Monteilhet, Cem. Concr. Res. (to be published).
[19] F. Barberon, J.-P. Korb, D. Petit, V. Morin, and E. Bermejo, Phys. Rev. Lett. **90**, 116103 (2003).
[20] J.-P. Korb, L. Monteilhet, P. J. McDonald, and J. Mitchell, Cem. Concr. Res. (to be published).
[21] L. Venkataramanan, Y. Q. Song, and M. D. Hurlimann, IEEE Trans. Signal Process. **50**, 1017 (2002).
[22] H. McConnell, J. Chem. Phys. **28**, 430 (1958).
[23] J. J. Fripiat, M. Letellier, and P. Levitz, Philos. Trans. R. Soc. London, Ser. A **311** 287 (1984).
[24] W. P. Halperin, J. Y. Jehng, and Y. Q. Song, Magn. Reson. Imaging **12**, 169 (1994).
[25] J. Israelachvili, *Intermolecular and Surface Forces*, 2nd Ed. (Academic Press, London, 1992).
[26] J.-P. Korb, M. Whaley-Hodges, Th. Gobron, and R. G. Bryant, Phys. Rev. E **60**, 3097 (1999).
[27] P. L. Pratt and H. M. Jennings, Annu. Rev. Mater. Sci. **11**, 123 (1981).
[28] J.-P. Korb, P. J. McDonald, L. Monteilhet, A. G. Kalinichev, and R. J. Kirkpatrick, Cem. Concr. Res. (to be published).